ECCOMAS Congress 2016
VII European Congress on Computational Methods in Applied Sciences and Engineering
M. Papadrakakis, V. Papadopoulos, G. Stefanou, V. Plevris (eds.)
Crete Island, Greece, 5–10 June 2016

EQUIVALENT SDOF MODEL FOR ESTIMATING BLAST-INDUCED DYNAMIC REACTIONS OF EQUILATERAL TRIANGULAR HARDENED WALL ELEMENTS

Sebastian Mendes[1], **Liling Cao**[1], **Douglas Heinze**[1], **Elisabeth Malsch**[1]

[1] Thornton Tomasetti
40 Wall Street, 19th Floor, New York, NY 10005-1304
e-mail: {SMendes, LCao, DHeinze, EMalsch}@ThorntonTomasetti.com

Keywords: Blast protection, blast-resistant wall, triangular plate, dynamic reaction, equivalent single degree-of-freedom system, elasto-plastic material, plate theory

Abstract. *Tall buildings oftentimes employ internal blast-resistant walls for protecting vital building areas and components from the damaging effects of high energy explosions. Architectural constraints may require hardened walls aligned with steel braced frames to be built in a shape equal to or near to that of an equilateral triangle. The analysis and design of the hardened walls and their supporting members for blast-induced dynamic loading is an imperative aspect of the design process. Parameters are derived for transforming the analysis of a simply-supported equilateral triangular hardened wall element subjected to blast loading into an equivalent single degree-of-freedom (SDOF) system. Expressions are then derived for obtaining the corresponding distributions of peak blast-induced dynamic reactions along the perimeter supports of the triangular wall element. The equivalent SDOF model and the expressions for the peak dynamic reaction distributions are subsequently validated with dynamic finite element analyses (FEA), therein verifying their applicability for rapidly analyzing and designing numerous quantities of equilateral triangular hardened wall elements and their supporting members in lieu of more rigorous and time-consuming dynamic FEA.*

1 INTRODUCTION

Tall buildings designed to resist high energy explosions oftentimes employ internal hardened walls for protecting means of egress and critical mechanical/electrical/plumbing (MEP) systems from blast infill pressures. For steel buildings with braced frame lateral systems, architectural constraints may require hardened walls to be subdivided into non-rectangular elements and supported in-plane of a building's braced frames. The magnitude and distribution of blast loads upon the braced frame as caused by blast-induced dynamic reactions of hardened walls are typically required for checking the performance and connection capacity of the individual braced frame members.

In this study a proposed equivalent SDOF model is developed for an equilateral triangular hardened wall element simply-supported in-plane of an inverted V-braced frame and uniformly loaded by blast infill pressure described by a linearly decaying pressure-time history *q(t)* (see Figure 1). Typical V-braced frames are constructed in a shape closer to that of a wide isosceles triangle. However, to simplify the analysis an equilateral triangle is chosen. The SDOF model is used to analyze the distribution of peak blast-induced dynamic reactions along the edges of triangular wall elements, and the results are validated with dynamic FEA. This verification indicates that the equivalent SDOF model can be practically incorporated into standard SDOF blast analysis spreadsheets for highly repetitive analysis and design of braced frame members supporting equilateral triangular hardened wall elements in-plane for blast.

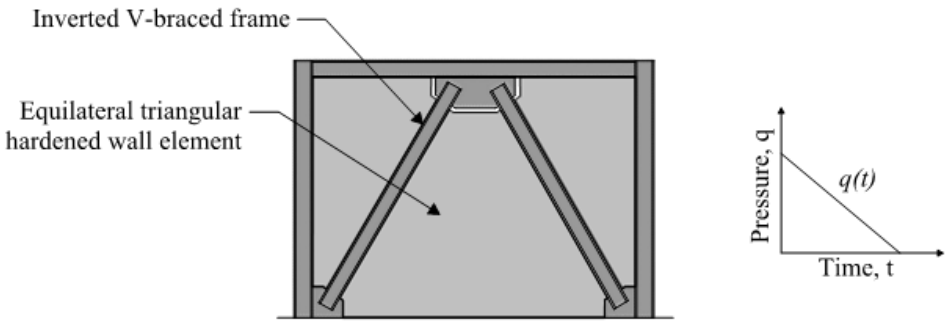

Figure 1: Equilateral triangular hardened wall element simply-supported in-plane of inverted V-braced frame and uniformly loaded by blast infill pressure.

2 EQUIVALENT SDOF MODEL FOR EQUILATERAL TRIANGULAR PLATE

2.1 SDOF Governing Equations of Motion

The equilateral triangular hardened wall element is assumed to behave as a homogeneous isotropic plate possessing elastic-perfectly plastic material properties (i.e. steel plate). The dynamic blast analysis of the real system, consisting of the equilateral triangular plate loaded by *q(t)*, is transformed into an equivalent undamped SDOF system subjected to an equivalent load-time history (see Figure 2). In the elastic phase the governing undamped equation of motion for the equivalent system is:

$$M_e \frac{d^2}{dt^2} z(t) + k_e z(t) = F_e(t) \tag{1}$$

where M_e and k_e are the equivalent mass and stiffness, respectively, in the elastic phase. Also, $z(t)$ is the real displacement and $F_e(t)$ is the equivalent load-time history in the elastic phase. In the plastic phase the equation of motion becomes:

$$M_p \frac{d^2}{dt^2} z(t) + R_m = F_p(t) \tag{2}$$

where R_m is the maximum resistance, and M_p and $F_p(t)$ are the equivalent mass and load-time history, respectively, in the plastic phase. The system converts to free vibration upon the termination of the load-time history.

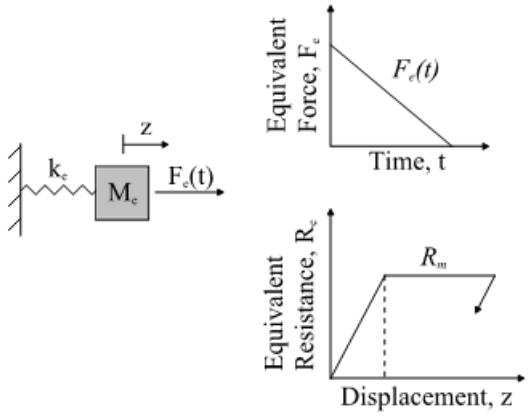

Figure 2: Equivalent SDOF system loaded by equivalent load-time history.

The real stiffness and maximum resistance of the equilateral triangular plate are required to develop the equivalent SDOF system. Also, the deflection surface, shape function, and transformation factors for the elastic and plastic phases are required to develop the equivalent SDOF system. Numerical analysis such as with the constant-velocity procedure allows for a solution of the response [1].

In the case of this study we are interested in the maximum displacement, z_{max}, of the system in the free vibration phase such that the peak dynamic reaction, Q_{max}, may be obtained from the constitutive relations:

$$Q_{\max} = \min \begin{cases} kz_{\max} \\ R_m \end{cases} \tag{3}$$

where k is the real stiffness. A third factor limiting the maximum dynamic reaction is the shear strength of the plate along its supported edges. In the case of this study the shear strength is assumed to exceed the dynamic shear demand. Using (3) the distribution of the peak dynamic reaction along the edges of the equilateral triangular plate may therein be determined using the plate deflection surface and constitutive equations. This distribution represents the peak blast-induced dynamic reaction of the equilateral triangular hardened wall element upon the supporting braced frame members.

2.2 Deflection Surface, Shape Function, and Stiffness in Elastic Phase

It is assumed that the deformed shape of the triangular plate during elastic response to blast loading conforms to the plate deflection surface obtained from a statically applied uniform surface load. Any deflection surface, *w(x,y)*, for a homogeneous plate must satisfy the governing plate equation:

$$\nabla^4 w(x,y) = \frac{\partial^4 w}{\partial x^4} + 2\frac{\partial^4 w}{\partial x^2 \partial y^2} + \frac{\partial^4 w}{\partial y^4} = \frac{q}{D} \tag{4}$$

where q is a uniform surface load and D is the plate flexural rigidity defined by $Et^3/[12(1-\nu^2)]$. The following deflection surface satisfies (4) for an equilateral triangular plate (see Figure 3a) simply-supported along the edges and uniformly loaded by q [2]:

$$w(x,y) = \frac{q}{64aD}\left[x^3 - 3y^2 x - a\left(x^2+y^2\right) + \frac{4}{27}a^3\right]\left(\frac{4}{9}a^2 - x^2 - y^2\right) \tag{5}$$

The deflection surface intrinsically includes the plate bending stiffness and applied surface load. The more general shape function, $\phi(x,y)$, describing the deflection surface independently of stiffness and load (see Figure 3b) is determined by extricating from (5) the plate bending stiffness explicit to the displacement at the center of the plate due to surface load q:

$$\phi(x,y) = \frac{243}{16a^5}\left[x^3 - 3y^2 x - a\left(x^2+y^2\right) + \frac{4}{27}a^3\right]\left(\frac{4}{9}a^2 - x^2 - y^2\right) \tag{6}$$

where the plate bending stiffness corresponding to the displacement at the center of the plate is solved to be:

$$k = \frac{324\sqrt{3}D}{a^2} \tag{7}$$

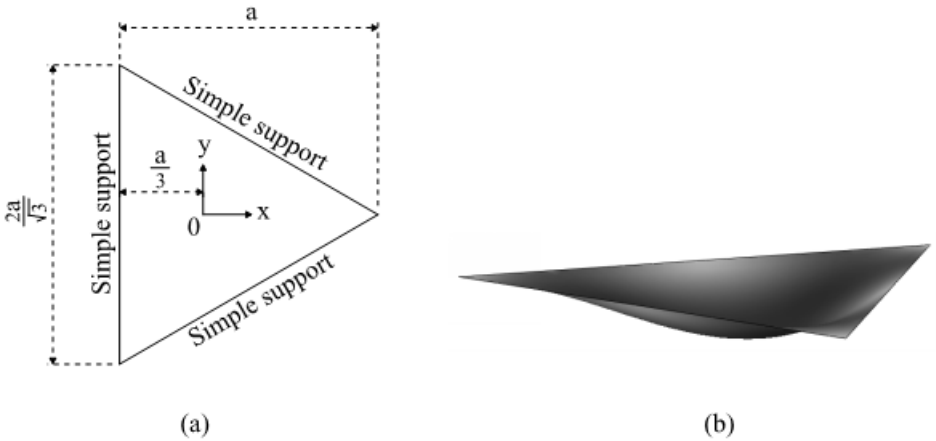

Figure 3: (a) Simply-supported equilateral triangular plate and (b) shape function in elastic phase.

2.3 Approximate Maximum Resistance

In accordance with yield line theory the maximum resistance of the equilateral triangular plate signifying the initiation of the plastic phase is defined by the formation of plastic hinges along the lines bisecting the angles of the triangle (see Figure 4). It is approximated that the formation of plastic hinges occurs when the von Mises stress, σ_v, along the bisecting lines achieves the yield stress, σ_Y. The elasto-plastic transition range leading to the true formation of plastic hinges is complex and has been ignored in this study. However, if the plate thickness is relatively thin compared to the area dimensions then the elasto-plastic range becomes exceedingly negligible [1].

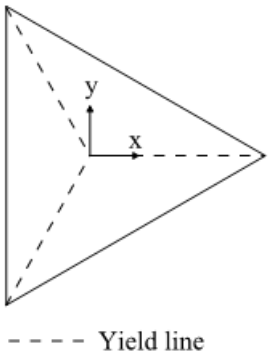

Figure 4: Yield lines on equilateral triangular plate.

An expression for the approximate maximum resistance requires a relation between the applied surface load and the von Mises stress along the yield lines. The plate constitutive equations relating bending moments to curvatures are written as follows [2]:

$$M_x(x,y) = D\left(\frac{\partial^2 w}{\partial x^2} + \nu\frac{\partial^2 w}{\partial y^2}\right) \qquad M_y(x,y) = D\left(\nu\frac{\partial^2 w}{\partial x^2} + \frac{\partial^2 w}{\partial y^2}\right) \qquad M_{xy}(x,y) = D(1+\nu)\frac{\partial^2 w}{\partial x \partial y} \tag{8}$$

where ν is Poisson's ratio. The plane stress components in turn are written in terms of the plate bending moments as:

$$\sigma_x(x,y) = \frac{6M_x}{t^2} \qquad \sigma_y(x,y) = \frac{6M_y}{t^2} \qquad \tau_{xy}(x,y) = \frac{6M_{xy}}{t^2} \tag{9}$$

The principal plane stress components σ_1 and σ_2 are defined in terms of the plane stress components as [3]:

$$\sigma_{1,2} = \frac{\sigma_x + \sigma_y}{2} \pm \sqrt{\left(\frac{\sigma_x - \sigma_y}{2}\right)^2 + \tau_{xy}^2} \tag{10}$$

Finally, the von Mises stress is defined in terms of the principal plane stress components as:

$$\sigma_v(x,y) = \sqrt{\sigma_1^2 - \sigma_1\sigma_2 + \sigma_2^2} \tag{11}$$

As a result, the von Mises stress at any location on the plate can be expressed in terms of the deflection surface given by (5) by sequentially substituting equations (8) through (10) into (11).

The onset of yielding along each yield line does not occur uniformly as demonstrated in Figure 5. The stress profile is approximately rectangular with the peak stress occurring at the center of the plate and sharply decreasing near the edge of the plate. It is therein approximated that uniform yielding along each yield line occurs when the peak von Mises stress at the center of the plate achieves the yield stress. The von Mises stress at the center of the plate is solved from (11) to be:

$$\sigma_v(0,0) = \frac{1}{9}\sqrt{\frac{(1+\nu)^2 a^4 q^2}{t^4}} \tag{12}$$

Setting $\sigma_v = \sigma_Y$ and solving for the maximum surface load q_m corresponding to yielding at the center of the plate results in:

$$q_m = \frac{9t^2\sigma_Y}{a^2(1+\nu)} \tag{13}$$

Furthermore, multiplying (13) by the area of the triangle results in an expression for the approximate maximum resistance:

$$R_m = \frac{3t^2\sigma_Y\sqrt{3}}{1+\nu} \tag{14}$$

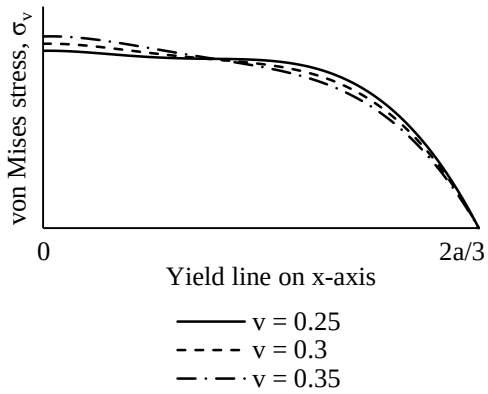

Figure 5: Plot of von Mises stress along yield line on x-axis.

2.4 Shape Function in Plastic Phase

In the plastic phase the plate resistance is R_m and the plate bending stiffness explicit to the displacement at the center of the plate vanishes. The corresponding shape function is assumed to take on the shape of a tetrahedron with its edges defined by the yield lines (see Figure 6). The presence of the edges disallows the use of a continuous shape function for describing the deflection surface over the entire triangular area. As an alternative, a one-dimensional linear shape function, $\Phi(x)$, describing any line in-plane of a tetrahedron face and oriented perpendicular to the perimeter edge can be defined and integrated over each face to obtain

corresponding transformation factors. The linear shape function projected parallel to the x-axis and originating along the perimeter edge at $x = -a/3$ is written as:

$$\Phi(x) = \frac{3x}{a} + 1 \tag{15}$$

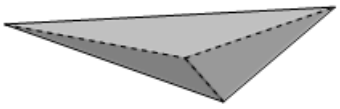

Figure 6: Tetrahedron shape function in plastic phase.

2.5 Transformation Factors

Transformation factors are derived to convert the mass, stiffness, resistance, and load-time history of the real system into equivalent values for use in the equivalent SDOF system, of which is governed by the equations of motion defined by (1) and (2). Transformation factors are obtained for the elastic and plastic phases by integrating the corresponding shape function over the surface of the plate [1]. In general, the mass factor is defined by:

$$K_M = \frac{\int\int^A m\phi^2(x,y)dxdy}{mA} \tag{16}$$

where m is the mass per unit area and A is the area of the triangle. Also, the load factor is defined by:

$$K_L = \frac{\int\int^A q\phi(x,y)dxdy}{qA} \tag{17}$$

Transformation factors for the elastic phase are obtained by integrating $\phi(x,y)$ over the surface of the plate. Integration over the triangular surface requires the limits of integration to vary as functions of the linear equations defining the perimeter of the triangle. Substituting (6) into (16) results in the mass factor for the elastic phase:

$$K_{M,e} = \frac{\int_{-\frac{a}{3}}^{\frac{2a}{3}} \int_{\frac{x\sqrt{3}}{3}-\frac{2a\sqrt{3}}{9}}^{-\frac{x\sqrt{3}}{3}+\frac{2a\sqrt{3}}{9}} m\phi^2(x,y)dydx}{\frac{ma^2\sqrt{3}}{3}} = 0.24 \tag{18}$$

Also, substituting (6) into (17) results in the load factor for the elastic phase:

$$K_{L,e} = \frac{\int_{-\frac{a}{3}}^{\frac{2a}{3}} \int_{\frac{x\sqrt{3}}{3}-\frac{2a\sqrt{3}}{9}}^{-\frac{x\sqrt{3}}{3}+\frac{2a\sqrt{3}}{9}} q\phi(x,y)\,dy\,dx}{\frac{qa^2\sqrt{3}}{3}} = 0.39 \tag{19}$$

Transformation factors for the plastic phase are obtained by integrating the one-dimensional linear shape function $\Phi(x)$ over one-sixth of the total plate area bounded by $x = -a/3$, $y = 0$, and the yield line along $y = x\sqrt{3}$. It is apparent that the considered area is representative of the remaining five divisions of plate area owing to the symmetry of an equilateral triangle. Integration over this area requires the limits of integration to vary as functions of the linear equations defining the yield line. By symmetry it is allowable to multiply the double integrals by six to obtain the final transformation factors. Substituting (15) into (16) results in the mass factor for the plastic phase:

$$K_{M,p} = \frac{6\int_{0}^{\frac{a\sqrt{3}}{3}} \int_{-\frac{a}{3}}^{-\frac{y\sqrt{3}}{3}} m\Phi^2(x)\,dx\,dy}{\frac{ma^2\sqrt{3}}{3}} = 0.17 \tag{20}$$

Also, substituting (15) into (17) results in the load factor for the plastic phase:

$$K_{L,p} = \frac{6\int_{0}^{\frac{a\sqrt{3}}{3}} \int_{-\frac{a}{3}}^{-\frac{y\sqrt{3}}{3}} q\Phi(x)\,dx\,dy}{\frac{qa^2\sqrt{3}}{3}} = 0.33 \tag{21}$$

The derived transformation factors, maximum resistance, and stiffness for the elastic and plastic phases are summarized in Table 1. The response of the equivalent SDOF system may therein be solved using the constant-velocity procedure [1] to obtain the maximum displacement z_{max} in the free vibration phase, from which the distribution of the peak dynamic edge reaction can be determined.

Strain range	Load factor, K_L	Mass factor, K_M	Real stiffness, k	Maximum resistance, R_m
Elastic	0.39	0.24	$\frac{324\sqrt{3}D}{a^2}$	$\frac{3t^2\sigma_Y\sqrt{3}}{1+\nu}$
Plastic	0.33	0.17	0	

Table 1: Parameters for equivalent SDOF model.

3 DISTRIBUTION OF PEAK DYNAMIC EDGE REACTION

Assuming the blast load duration is much shorter than the period of response for the plate element, the distribution of the peak dynamic reaction along the edges of the equilateral triangular plate is dependent upon the dynamic response of the system during the free vibration phase; if the system remains elastic then the reaction distribution is derived from the elastic deflection surface given by (5) and the peak response z_{max}. Conversely, if the system becomes plastic then the reaction distribution is derived from the tetrahedron shape function and R_m.

3.1 Edge Reaction Distribution in Elastic Phase

The distribution of the peak dynamic reaction for the elastic phase is first developed. The edge reaction distribution requires a relation between z_{max} in the free vibration phase and the corresponding plate shear force, $Q_i(x,y)$, at any location on the plate. It is apparent that the shear force distribution along the perimeter edges corresponding to z_{max} is identical to the peak dynamic edge reaction. The plate shear force is related to the plate bending moments by [2]:

$$Q_x(x,y) = \frac{\partial M_x}{\partial x} + \frac{\partial M_{xy}}{\partial y} \qquad Q_y(x,y) = \frac{\partial M_{xy}}{\partial x} + \frac{\partial M_y}{\partial y} \tag{22}$$

Sequentially substituting (5) and (8) into $(22)_1$ and setting $x = -a/3$ results in an expression for the edge reaction distribution along the perimeter edge parallel to the y-axis due to uniform surface load q:

$$Q_{x,eu}\left(-\frac{a}{3}, y\right) = -\frac{q}{8a}\left(2a^2 - 6y^2 + \nu a^2 - 9\nu y^2\right) \tag{23}$$

The force developed into the perimeter edge supports during the free vibration phase is derived from the inertia force. The distribution of the inertia force across the plate surface is non-uniform and is proportional to the deflection surface. As a result, the edge reaction distribution given by (23) must be scaled by a ratio, α, of the uniform surface load q_E corresponding to the peak displacement z_{max} at the center of the plate, and an equivalent surface load $r_E(x,y)$ proportional to $\phi(x,y)$. The equivalent surface load $r_E(x,y)$ represents the inertia force imposed upon the plate.

The uniform surface load q_E corresponding to z_{max} is solved from (5) to be:

$$q_E = \frac{972 D z_{\max}}{a^4} \tag{24}$$

Conversely, the equivalent surface load $r_E(x,y)$ is expressed in terms of a unit uniform surface load q_u and a constant C_e which controls the amplitude of $\phi(x,y)$ at the center of the plate:

$$r_E(x,y) = q_u C_e \phi(x,y) \tag{25}$$

The total force imposed by $r_E(x,y)$ upon the plate must be equivalent to the total force developed into the perimeter edge supports corresponding to z_{max}. The constant C_e is determined by integrating $r_E(x,y)$ over the surface of the triangular plate and equating the result with the total force derived from the constitutive relation corresponding to z_{max}:

$$q_u C_e \int_{-\frac{a}{3}}^{\frac{2a}{3}} \int_{\frac{x\sqrt{3}}{3}-\frac{2a\sqrt{3}}{9}}^{-\frac{x\sqrt{3}}{3}+\frac{2a\sqrt{3}}{9}} \phi(x,y)\,dy\,dx = kz_{\max} \tag{26}$$

where the limits of integration vary as functions of the linear equations defining the perimeter of the triangular plate. Substituting (6) and (7) into (26), resolving the integral, solving for C_e, and substituting the result into (25) gives an expression for the equivalent surface load:

$$r_E(x,y) = \frac{2520 D z_{\max}}{a^4}\phi(x,y) \tag{27}$$

The ratio α is developed by considering the forces per unit length, Q_E and R_E, developed into a perimeter edge as derived from surface loads q_E and $r_E(x,y)$, respectively, within the corresponding tributary width (see Figure 7). The boundaries delineating the tributary width of each perimeter edge are coincident with the assumed yield lines. Considering the tributary area bounded by $x = -a/3$, $y = 0$, and the yield line along $y = x\sqrt{3}$, the ratio α is defined as follows:

$$\alpha(y) = \frac{R_E(y)}{Q_E(y)} \tag{28}$$

where $Q_E(y)$ and $R_E(y)$ are the forces per unit length developed into the perimeter edge along $x = -a/3$. It is apparent that the magnitudes of $Q_E(y)$ and $R_E(y)$ are represented by the areas beneath q_E and $r_E(x,y)$ at any section parallel to the x-axis between $y = 0$ and $y = a\sqrt{3}/3$, and within the domain bounded by $x = -a/3$ and $x = -y\sqrt{3}/3$ (see Figure 8). The force per unit length as derived from q_E is solved to be:

$$Q_E(y) = q_E\left(\frac{a}{3} - \frac{y\sqrt{3}}{3}\right) \tag{29}$$

Also, the force per unit length as derived from $r_E(x,y)$ is defined by:

$$R_E(y) = \int_{-\frac{a}{3}}^{-\frac{y\sqrt{3}}{3}} r_E(x,y)\,dx \tag{30}$$

where the limits of integration vary as functions of the linear equations defining the yield lines.

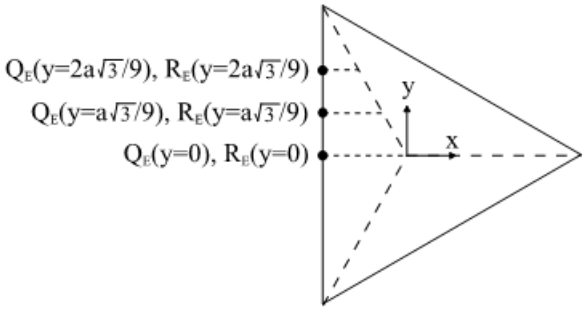

Figure 7: Forces per unit length $Q_E(y)$ and $R_E(y)$ developed into the perimeter edge along $x = -a/3$.

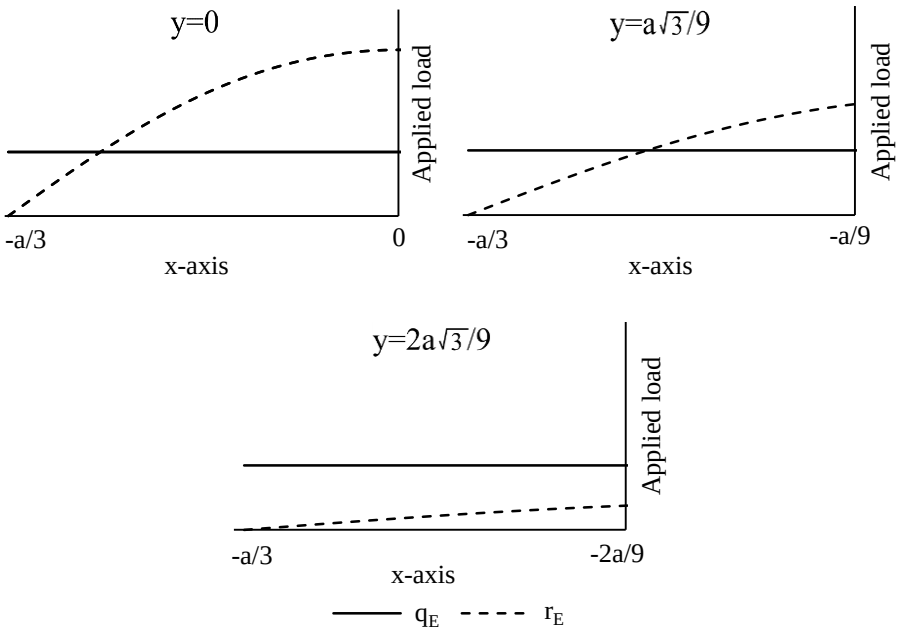

Figure 8: Plots of surface loads q_E and r_E tributary to the perimeter edge along $x = -a/3$.

Substituting (24) into (23) and multiplying the result by $\alpha(y)$ gives an expression for the peak dynamic edge reaction distribution during the elastic phase in terms of z_{max} along the edge at $x = -a/3$ and within the domain bounded by $y = 0$ and $y = a\sqrt{3}/3$:

$$Q_{x,e}\left(-\frac{a}{3}, y\right) = -\alpha(y)\frac{81Et^3 z_{\max}}{8a^5\left(\nu^2 - 1\right)}\left(2a^2 - 6y^2 + \nu a^2 - 9\nu y^2\right) \tag{31}$$

Full substitution of (28) into (31) results in an extensive formula and is not explicitly shown here. It is apparent that this distribution is mirrored in the domain bounded by $y = -a\sqrt{3}/3$ and $y = 0$. Also, the distribution is identical along the other two perimeter edges.

3.2 Edge Reaction Distribution in Plastic Phase

In the plastic phase the peak dynamic reaction Q_{max} is capped by the maximum resistance R_m expressed by (14). The corresponding edge reaction distribution is derived by disseminating an equivalent surface load $p_E(x,y)$ possessing a total magnitude equal to R_m in accordance with the tributary width of each perimeter edge. The boundaries delineating the tributary width of each perimeter edge are coincident with the assumed yield lines. The distribution of $p_E(x,y$ across the plate is proportional to the tetrahedron shape function described by $\Phi(x)$ and represents the capped inertia force imposed upon the plate during the plastic phase.

Considering the tributary area bounded by $x = -a/3$, $y = 0$, and the yield line along $y = x\sqrt{3}$, the equivalent surface load $p_E(x,y)$ is expressed in terms of the unit uniform surface load q_u and a constant C_p which controls the amplitude of $\Phi(x)$ at the center of the plate:

$$p_E(x,y) = q_u C_p \Phi(x) \tag{32}$$

It is apparent that the considered tributary area is representative of the remaining five divisions of plate tributary area because of the symmetry of an equilateral triangle. Therefore, the force imposed by $p_E(x,y)$ upon the plate within the considered tributary area must be equivalent to one-sixth of the maximum resistance R_m. The constant C_p is determined by integrating $p_E(x,y)$ over the surface of the considered tributary area and equating the result with one-sixth of R_m:

$$q_u C_p \int_0^{\frac{a\sqrt{3}}{3}} \int_{-\frac{a}{3}}^{-\frac{y\sqrt{3}}{3}} \Phi(x)\,dx\,dy = \frac{R_m}{6} \tag{33}$$

where the limits of integration vary as functions of the linear equations defining the yield lines. Substituting (14) and (15) into (33), resolving the integral, solving for C_p, and substituting the result into (32) gives an expression for the equivalent surface load:

$$p_E(x,y) = \frac{27t^2\sigma_Y}{a^2(1+\nu)}\Phi(x) \tag{34}$$

The dissemination of $p_E(x,y)$ into the perimeter edge along $x = -a/3$ is expressed by:

$$Q_{x,p}\left(-\frac{a}{3}, y\right) = \int_{-\frac{a}{3}}^{-\frac{y\sqrt{3}}{3}} p_E(x,y)\,dx \tag{35}$$

where the limits of integration vary as functions of the linear equations defining the yield lines. Sequentially substituting (15) and (34) into (35) and resolving the integral results in an expression for the dynamic edge reaction distribution during the plastic phase along the edge at $x = -a/3$ and within the domain bounded by $y = 0$ and $y = a\sqrt{3}/3$:

$$Q_{x,p}\left(-\frac{a}{3}, y\right) = -\frac{9t^2\sigma_Y}{2a^3(1+\nu)}\left(-3y^2 - a^2 + 2ay\sqrt{3}\right) \tag{36}$$

It is apparent that this distribution is mirrored in the domain bounded by $y = -a\sqrt{3}/3$ and $y = 0$. Also, the distribution is identical along the other two perimeter edges.

4 VALIDATION WITH DYNAMIC FINITE ELEMENT ANALYSES

4.1 Analytical Setup and Equivalent SDOF Analysis

The distribution of peak blast-induced dynamic reactions along the edges of three steel plate wall elements are determined using the equivalent SDOF model together with (31) and (36). The resulting reaction distributions are verified with dynamic FEA using ABAQUS/CAE. The three steel plate wall elements are assumed to be positioned within the braced frame lateral system of an imaginary 10-story building as shown in Figure 9. Each wall element is simply-supported in-plane of an inverted V-braced frame as shown in Figure 10a. Furthermore, each wall element is assumed to be formed in the shape of an equilateral triangle. It is noted that only equilateral triangular wall elements are assessed; other non-rectangular wall elements are deemed beyond the scope of this study but are considered no less important.

The wall elements are designed to protect the building's MEP systems from an assumed external street threat equivalent to the explosion of 1100 kg of TNT. The equivalent uniform peak pressure and impulse imposed upon each wall element are obtained using the blast effects software ConWep (see Table 2). The blast infill pressure is assumed to be described by a linearly decaying pressure-time history *q(t)* as shown in Figure 10b and does not account for the façade or any shielding by the floor slabs. The equivalent SDOF model is used to design the wall elements to meet the performance criteria recommended by ASCE 59-11 *Blast Protection of Buildings* [4] for moderate damage. Namely, the parameters summarized in Table 1 are used to develop an equivalent SDOF system for each wall element and the response of the system is solved for using the constant-velocity procedure [1]. Final wall element thicknesses are converged upon through iteration. The resulting geometric and material properties of each wall element are summarized in Tables 3 and 4, respectively. The resulting peak out-of-plane displacements at the center of each wall element during the free vibration phase are summarized in Table 5.

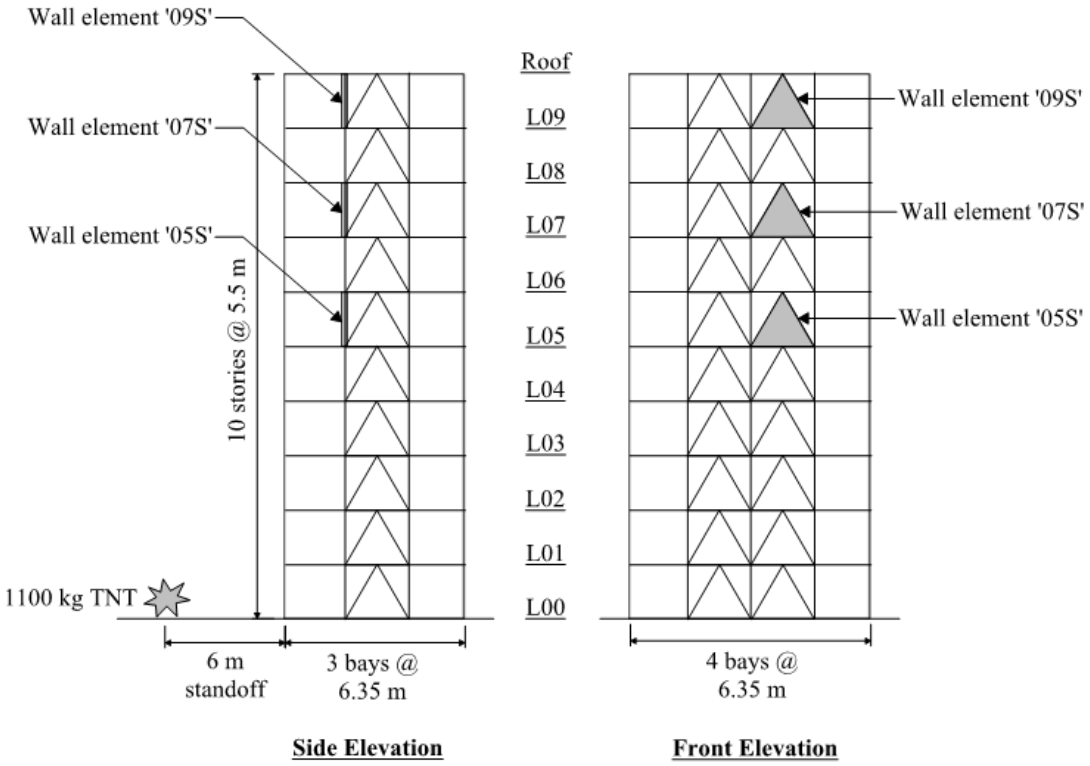

Figure 9: Imaginary 10-story building with steel plate wall elements in-plane of braced frame.

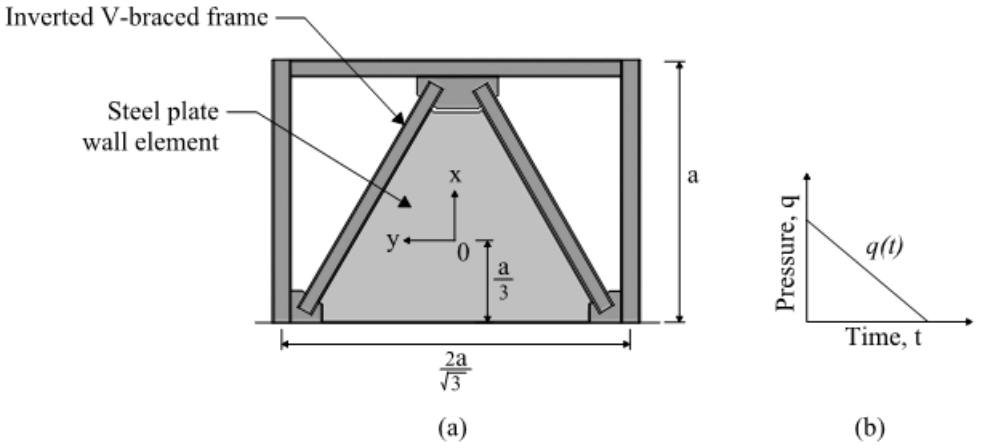

Figure 10: (a) Steel plate wall element loaded by (b) linearly decaying pressure-time history.

Wall element	Range to blast (m)	Uniform peak pressure (kPa)	Uniform impulse (kPa-msec)
05S	36	145	1158
07S	47	76	848
09S	58	48	669

Table 2: Blast pressure and impulse imposed on each wall element.

Wall element	Material[1]	Height (m)	Width (m)	Thickness, t (cm)
05S	Steel plate	5.5	6.35	4.5
07S	Steel plate	5.5	6.35	4.0
09S	Steel plate	5.5	6.35	3.5

1. Refer to Table 4 for material properties.

Table 3: Wall element geometric properties.

Material	Yield strength, σ_Y (MPa)	Young's modulus, E (GPa)	Poisson's ratio, v	Density, ρ (kg/m^3)
Steel plate	250	200	0.30	7860

Table 4: Wall element material properties [3].

Wall element	Peak SDOF response, z_{max} (cm)	Rotation, θ	Ductility, μ	Rotation response limit, θ_{max}	Ductility response limit, μ_{max}
05S	5.8	1.82˚	0.90		
07S	5.2	1.63˚	0.71	2˚	8
09S	5.3	1.65˚	0.63		

Table 5: Peak SDOF responses and ASCE 59-11 response limits for steel plates considering moderate damage [4].

4.2 FEA Setup and Analysis

The three steel plate wall elements are modeled in ABAQUS/CAE in accordance with the geometric and material properties specified in Tables 3 and 4, respectively. Triangular shell elements are used to mesh the geometry, and simple supports are applied to the perimeter edges of each modeled wall element (see Figure 11). A finer mesh is developed in the vicinity of the three corner regions. Zero damping is assigned to the section properties.

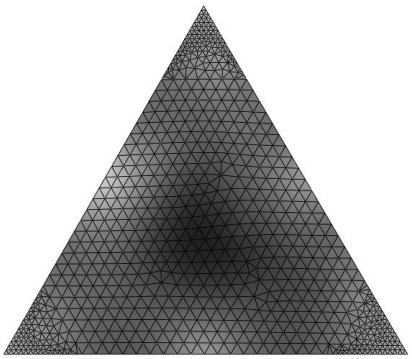

Figure 11: Typical steel plate wall element as modeled in ABAQUS.

The dynamic analysis for each wall element is carried out in two steps. First, an implicit dynamic load step is executed in which a uniform pressure is applied to the wall element. The uniform pressure is described by a linearly decaying ramp function (see Figure 10b) formulated in accordance with the pressure-time history described by the equivalent uniform peak pressure and impulse specified in Table 2. A second implicit dynamic load step is next performed in the absence of external loading to model the free vibration phase. History output requests are obtained at each time step for the out-of-plane nodal displacements and edge reactions.

Displacement-time history plots of the out-of-plane displacement at the center of each wall element as obtained from FEA and the equivalent SDOF system are displayed in Figure 10. The time history is displayed from the initial response to the blast infill pressure to 200 msec. The FEA and SDOF time history plots demonstrate very good correspondence.

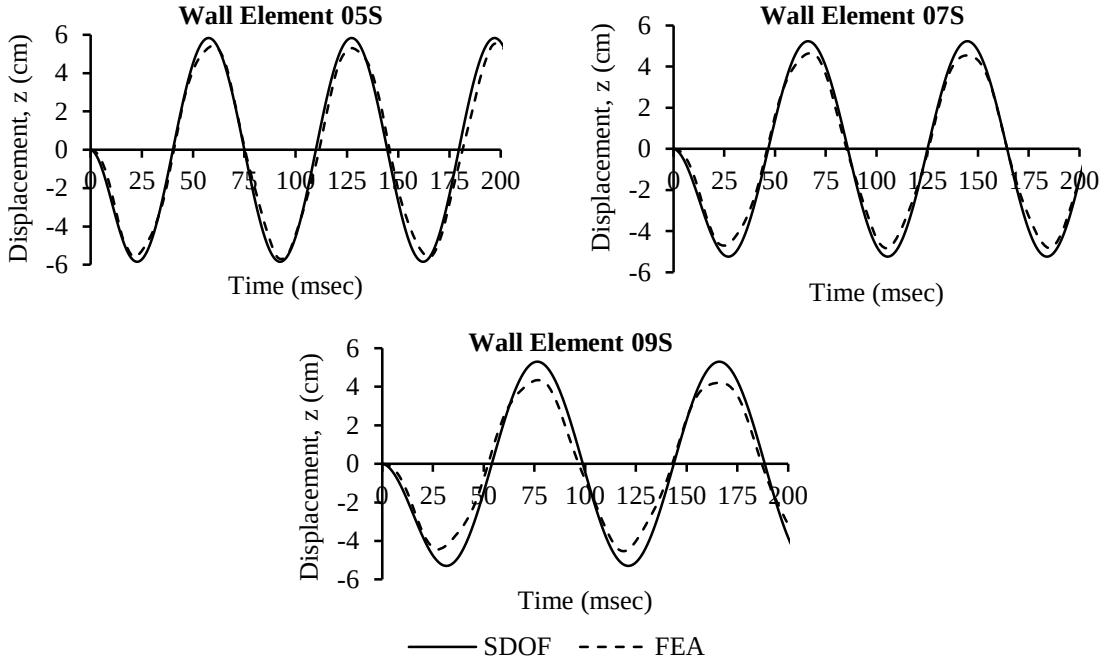

Figure 10: Displacement-time history plots of the out-of-plane displacement at the center of each wall element as obtained from SDOF and FEA.

4.3 Distribution of Peak Dynamic Edge Reaction

The responses of all three steel plate wall elements remain elastic throughout the free vibration phase (i.e. ductility, $\mu < 1.0$). As a result, the peak dynamic edge reaction distribution is determined using (31). Substituting into (31) the geometric and material properties listed in Tables 3 and 4, and the peak responses summarized in Table 5, allows for the computation of the peak dynamic edge reaction distribution for each wall element along the edge located at $x = -a/3$ and between $y = 0$ and $y = a\sqrt{3}/3$ (see Figure 11). The resulting edge reaction distribution is representative of the distributions along the remaining five edge segments owing to the symmetry of an equilateral triangle and the uniform blast infill pressure.

The peak dynamic edge reaction distribution for each wall element during the free vibration phase is determined in ABAQUS/CAE by way of three steps. First, a nodal path is created along an edge of each wall element. Specifically, the edge located at $x = -a/3$ and between $y = 0$ and $y = a\sqrt{3}/3$ is investigated. Next, the time step of peak displacement during the free vibration phase is determined from the displacement-time history plots. Finally, the edge reaction distribution along the nodal path is obtained from the history output requests at the time step of peak displacement (see Figure 11). The peak dynamic edge reaction distribution for each wall element as obtained from FEA and (31) demonstrates good correspondence.

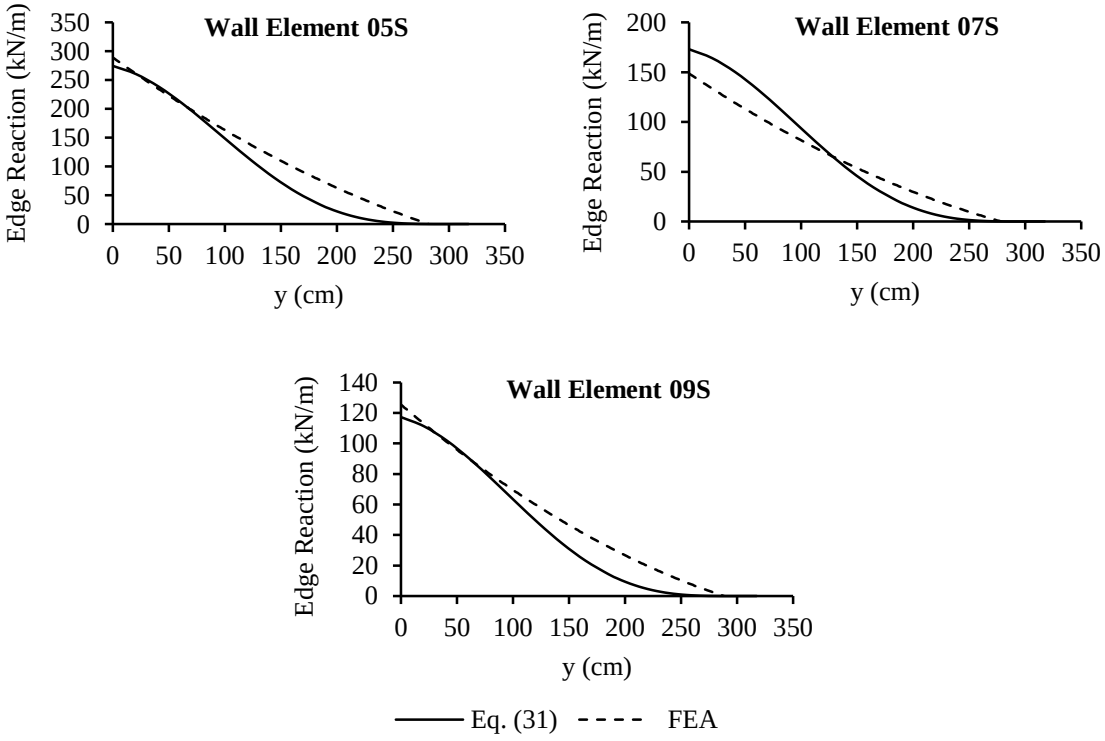

Figure 11: Time history plots of the out-of-plane displacement at the center of each wall element as obtained from SDOF and FEA.

5 CONCLUSIONS

Classical plate theory and mechanics of materials were employed to develop an equivalent SDOF model for describing the dynamic response of an equilateral triangular hardened wall element simply-supported in-plane of an inverted V-braced frame and uniformly loaded by blast infill pressure. Expressions (31) and (36) were then derived using the aforementioned theories for describing the distribution of the peak dynamic edge reactions along the perimeter supports of the wall element. The equivalent SDOF system and (31) were subsequently validated with dynamic FEA using ABAQUS/CAE.

The process of designing the lateral system of a tall building for wind and seismic loads is made more complex by also having to analyze and design individual braced frame members for out-of-plane blast loads as caused by blast-induced dynamic reactions of hardened walls. The presence of numerous quantities of hardened walls and supporting braced frame members within the tall building may make impractical the use of dynamic FEA for analyzing and designing the walls and braced frame members. The parameters summarized in Table 1 are highly applicable in that they may be easily incorporated into standard SDOF blast analysis spreadsheets for rapidly analyzing the dynamic response of hardened wall elements built in a form equal to or near to that of an equilateral triangle. The final design of wall elements may be refined by adjusting the wall geometric and material properties until an optimal design is converged upon through iteration. Importantly, the corresponding distributions of peak blast-induced dynamic reactions along the perimeter supports of wall elements, given by (31) and (36), may be used to efficiently analyze and design the supporting braced frame members.

Although this study dealt with homogeneous and isotropic equilateral triangular wall elements possessing elastic-perfectly plastic material properties, this work can indubitably be amended and expanded to include non-isotropic or non-homogeneous walls, such as reinforced concrete or stud walls. This would certainly involve modification of the assumed deformed shapes and out-of-plane stiffness. Closed-form solutions for wall elements built in the form of other non-rectangular shapes, such as wide isosceles triangles or right triangles, are increasingly complex. However, the analysis of an equilateral triangle is expected to envelop many cases seen in tall buildings.

REFERENCES

[1] J.M. Biggs, *Introduction to structural dynamics*. McGraw-Hill, 1964.

[2] S. Timoshenko, S. Woinowsky-Krieger, *Theory of plates and shells, 2nd Edition*. McGraw-Hill, 1987.

[3] F.P. Beer, E.R. Johnston, Jr., J.T. DeWolf, *Mechanics of Materials, 4th Edition*. McGraw-Hill, 2006.

[4] ASCE 59-11, *Blast Protection of Buildings*. American Society of Civil Engineers, 2011.